Available online at www.sciencedirect.com
SCIENCE DIRECT®
Physica B 339 (2003) 105–109
PHYSICA B
www.elsevier.com/locate/physb

First-principles study of La–$B_{36}N_{36}$ cage

Q. Wang[a,b,*], Q. Sun[b], T. Oku[c], Y. Kawazoe[a]

[a] *Institute for Materials Research, Tohoku University, Sendai 980-77, Japan*
[b] *Physics Department, Virginia Commonwealth University, 1020 West Main Street, Richmond, VA 23284, USA*
[c] *ISR, Osaka University, Osaka 567-0047, Japan*

Received 10 February 2003; received in revised form 17 July 2003; accepted 21 August 2003

Abstract

Based on the experimental studies of La–$B_{36}N_{36}$ cluster (Takeo Oku et al., Diamond Rel. Mater. 11 (2002) 940), first principles calculations using the projector-augmented wave method are performed on La–$B_{36}N_{36}$ cluster. The structure is fully optimized. It is found that the encapsulation of a La atom inside the $B_{36}N_{36}$ cage is energetically favorable, although the interaction between the La atom and the cage is weak. In order to optimize the interactions with the cage, the La atom is shifted off the cage center. The HOMO–LUMO gap is much reduced by doping, and the complex cage carries a magnetic moment of $1.0\mu_B$.

PACS: 61.46.+w; 36.40.Cg; 71.20.Tx; 61.48.+c

Keywords: First-principles calculations; La–$B_{36}N_{36}$ cage

1. Introduction

The discovery of the C_{60} [1] and carbon nanotubes [2] stimulated greatly the interest for nanostructures. Besides the carbon-based nanosystems, scientists also made extensions to other elements. B–N nanostructures are good examples. Classically, it is well known that the borazine $B_3N_3H_6$ is the analog of benzene C_6H_6, and the layered structure of honeycomb boron nitride (h-BN) is the analog of graphite. Therefore, due to the similarity between B–N and C–C units, a lot of effort has been devoted to boron-nitride (BN) fullerenelike materials (cluster, onions, intercalation, nanopolyhedra, nanotubes, and nanocapsules) in recent years, which have excellent properties such as heat resistance, insulation and structural stability [3,4]. Experimentally, the nested concentric BN polyhedrons have been successfully synthesized by reaction of BCl_3 with NH_3 in a laser beam [5]; A method to synthesize pure boron-nitride nanotubes was reported [3]. An isolated single-shelled BN fullerene with overall dimensions of 9–10 Å was formed by electron beam irradiation, and the octahedron model for these clusters was verified by high-resolution electron microscopy (HREM) [6]. Meanwhile, theoretical investigations have also been carried out on boron-nitride fullerenes [7–10] to

*Corresponding author. Physics Department, Virginia Commonwealth University, 1020 West Main Street, Richmond, VA 23284, USA. Tel.: 804-828-7079; fax: 804-828-7073.
E-mail address: qwang@vcu.edu (Q. Wang).

0921-4526/$ - see front matter © 2003 Elsevier B.V. All rights reserved.
doi:10.1016/j.physb.2003.08.119

understand their relative stability and size dependence of the properties. It has been found that for any value of $x \geqslant 4$ with the exception of $x = 5$, the $(BN)_x$ cages are made up of x-4 hexagons and 6 squares, the latter replace the 12 pentagons of carbon fullerene. The high stability of these clusters was found to correlate with a large HOMO–LUMO gap.

Recently doping of atoms in boron-nitride fullerenes was used as a way to synthesize new clusters, an endohedral BN fullerenelike La–$B_{36}N_{36}$ [11] was produced by one of the authors. A HREM image simulation has shown a possible existence of the La atom inside the $B_{36}N_{36}$ cage, and semi-empirical calculations were also reported [11]. However, La is a quite heavy element, the semi-empirical method used in Ref. [11] is not good for it. In this paper we study this system using density functional theory. The questions we are concerned are following: How does the La atom change the geometry and the electronic structure? What is the equilibrium position of La atom in the cage (i.e. in the center or off the center)? Does the cage carry a spin?

2. Theoretical method

We performed ab initio calculations using an iterative solution of the Kohn–Sham equations of the density-functional theory, based on the minimization of the norm of the residual vector of each eigenstate and an efficient charge density mixing [12,13]. For the exchange-correlation functional, gradient-corrected functionals in the form of the generalized gradient approximation (GGA) [14] have been chosen. A plane-wave basis set is adopted with the projector-augmented wave (PAW) method originally developed by Blöch [15] and recently adapted by Kresse and Joubert [16]. The particular advantage of the PAW method over the ultrasoft pseudo-potentials is that it can improve the accuracy especially of magnetic systems and materials including early d-elements or f-electron elements. In our calculations, the clusters are placed in a cubic cell with an edge length of 21 Å, keeping a distance about 12.5 Å between atoms in neighboring clusters, which is sufficiently large to make the dispersion effects negligible. In such a big supercell only the Γ point is used to represent the Brillouin zone. The cutoff energy for plane wave is 400 eV, the structure optimization is symmetry unrestricted, and the conjugate-gradient algorithm has been chosen. The optimization is terminated when all the forces acting on the atoms are less than 0.01 eV/Å. Due to the existence of a La atom in the La–$B_{36}N_{36}$ cluster, the calculations are performed with spin polarization.

3. Results and discussions

As a test of the computational method, we first performed calculations for a pure $B_{36}N_{36}$ fullerene taking the octahedron geometry reported in Ref. [10] as the starting configuration, which consists of 36 BN pairs distributed in six four-membered rings and 32 six-membered rings. The optimized structure is shown in Fig. 1(a), and it has T_d symmetry. The average binding energy per atom and the highest occupied and lowest unoccupied (HOMO–LUMO) gap are 8.4789 and 4.9296 eV, respectively. The average B–N bond length is 1.463 Å, and the average cage radius is 3.939 Å. In the four-membered rings, the average length of the B–N bond is 1.468 Å, the average B–N–B angle is 77.59° and the average N–B–N angle is 99.90°, as shown in Table 1. The results agree with previous ab initio calculations [10].

For the geometry of La–$B_{36}N_{36}$, we choose three initial structures for optimization. In the first one the La atom is put in the center of the $B_{36}N_{36}$ cage, while in the second and the third, the La atom is shifted the cage center by 0.5 and 1.0 Å, respectively. After optimization, the three initial structures converge to the same one; the cluster acquires C_s symmetry and the La atom is located at about 1.18 Å away from the center of the $B_{36}N_{36}$. The semi-empirical calculations gave a value of 0.02 Å [11], the La atom was predicted to be nearly in the cage center. However, the average cage radius is 3.94 Å which is much larger than the sum of the atomic radi of La and B(N) atoms. Therefore, to optimize the interactions with the

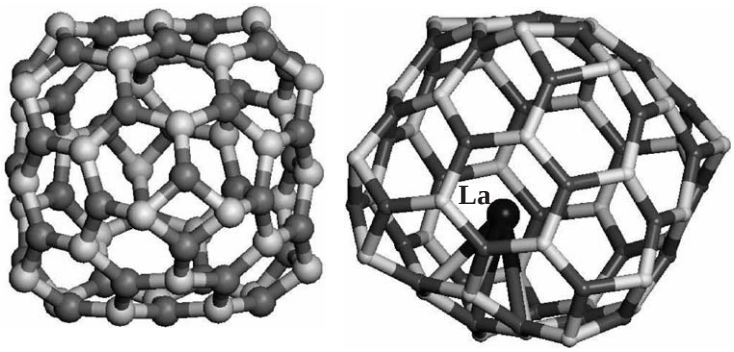

(a) (b)

Fig. 1. Structure of $B_{36}N_{36}$ (a) and La–$B_{36}N_{36}$ (b).

Table 1
The structure parameters for $B_{36}N_{36}$ and La–$B_{36}N_{36}$ clusters with T_d and C_s symmetries, respectively

Parameter	$B_{36}N_{36}$	La–$B_{36}N_{36}$
R_{B-N}	1.463	1.467
R_{S-C}	3.938	4.059
r_{B-N}	1.468	1.474
∠BNB	77.58	77.84
∠NBN	99.90	99.68

R_{B-N} represents the average B–N bond length, R_{S-C} stands for the average cage radius. r_{B-N}, ∠BNB and ∠NBN represent the average bond length and bond angles in four-remembered rings.

cage, the La atom has to shift off the cage center. In fact, the La atom is found to reside on one hexagonal ring of the $B_{36}N_{36}$ cage, as shown in Fig. 1(b). The distance between the La and the nearest-neighboring B and N atoms are 2.629, 2.608 Å, respectively, which are comparable with the sum of atomic radi of La–B and La–N. There is no noticeable change in the B–N bond lengths with the doping of the La atom, the average B–N bond length is just increased by 0.27% from 1.463 to 1.467 Å. The average cage radius is increased by 3.07% from 3.938 to 4.059 Å.

In order to check the stability of La–$B_{36}N_{36}$, we define the doping energy as the difference between the total energy of La–$B_{36}N_{36}$ and the sum of the total energies of the isolated La atom and the $B_{36}N_{36}$ cage, i.e., $E_{doping} = E(La-B_{36}N_{36})-[E(B_{36}N_{36}) + E(La)]$, which gives the doping energy of −0.8883 eV (about −20.5 kcal/mol). It shows that the reaction $La + B_{36}N_{36} \rightarrow La–B_{36}N_{36}$ is exothermic, and the production of La–$B_{36}N_{36}$ is energetically favorable. Thus La–$B_{36}N_{36}$ can be synthesized under appropriate condition, in agreement with the experimental success of the synthesis.

La–$B_{36}N_{36}$ is found to carry a magnetic moment of $1.0\mu_B$. To confirm the magnetic stability, the spin gaps are defined as

$$\delta_1 = -(\varepsilon^{+}_{HOMO} - \varepsilon^{-}_{LUMO}), \quad (1)$$

$$\delta_2 = -(\varepsilon^{-}_{HOMO} - \varepsilon^{+}_{LUMO}) \quad (2)$$

where + represents spin up and − spin down. The spin gap corresponds to the energy required to move an infinitesimal amount of charge from the HOMO of one spin to the LUMO of the other. Positive values for both spin gaps can guarantee that the system is stable magnetically and electronically. For La–$B_{36}N_{36}$, $\delta_1 = 0.4653$ eV, and $\delta_2 = 0.4610$ eV. While the HOMO–LUMO gap is 0.3664 eV, which is greatly reduced as compared to the empty cage of $B_{36}N_{36}$, as shown in Fig. 2. The gap we get is much larger than the semi-empirical values (0.0246 eV [11]). Therefore, doping with La makes the cage chemically more reactive. Where are the favorable reactive sites? Fig. 3 shows the frontier orbitals of the HOMO and LUMO. We can see that the HOMO is localized at the sites near the La atom, and the LUMO is localized on the La atom and on the B(N) atoms close to it. Therefore, the cage sites close to the La atom might be active in chemical

reaction. While for the empty $B_{36}N_{36}$ cage, the HOMO is mainly localized on the cage surface, and the LUMO is partly localized inside the cage, which results in the preferable encapsulation of La atom.

There is no evident charge transfer between the La atom and the B–N cage, different from the fullerene case. In C_{60} cage, low lying electron acceptor states (e.g., t_{1u}) exist, and these levels become populated by electrons from metal atom. However, BN cage has large gap with no electron acceptor states, charge transfer to the cage is not preferable. Accordingly, the interactions between the La atom and the $B_{36}N_{36}$ cage are weak. Fig. 4

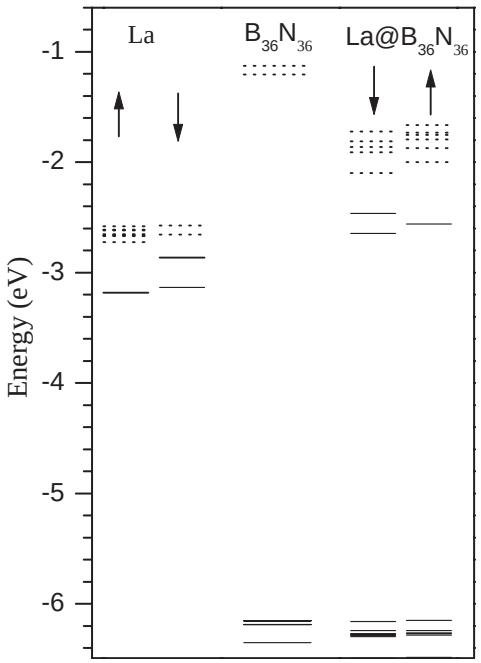

Fig. 2. Eigenvalue spectra for La, $B_{36}N_{36}$, and La–$B_{36}N_{36}$. The solid lines are for occupied states, and the dotted lines for unoccupied states.

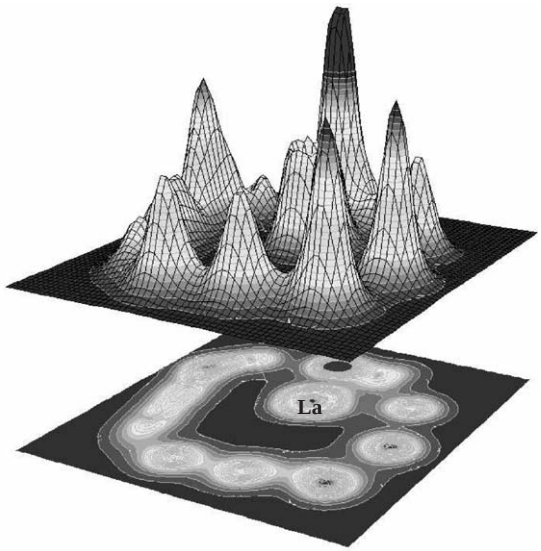

Fig. 4. The electron distribution of La–$B_{36}N_{36}$ on a plane through La and its nearest-neighboring B and N atoms. The contour lines are drawn from 0.001 ($e/Å^{-3}$) with 0.1 ($e/Å^{-3}$) step width.

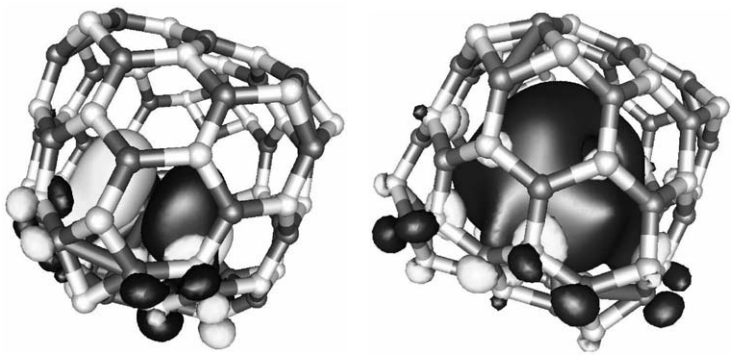

(a) (b)

Fig. 3. The frontier orbital of the HOMO (a) and the LUMO (b) of La–$B_{36}N_{36}$ with C_s symmetry, where the corresponding isosurface values are 0.02. Yellow is for positive, and blue for negative.

shows the charge distributions in the plane containing La and its two nearest B and N atoms.

In summary, we have reported studies on the metal-encapsulated boron-nitride fullerenelike cluster La–$B_{36}N_{36}$ by using first principles method. Compared to the semi-empirical calculations, some new results are obtained: (1) The La atom is about 1.18 Å shifted from the cage center; (2) The HOMO–LUMO gap for the doped cage is 0.366 eV; (3) The doped cage carries the magnetic moments of $1.0\mu_B$. (4) There is no charge transfer between the La atom and the $B_{36}N_{36}$ cage, resulting in a weak interaction.

Acknowledgements

The authors would like to express their sincere thanks to the crew of the Center for Computational Materials Science of the Institute for Materials Research, Tohoku University, for their continuous support of the HITAC SR-8000/G1-64 supercomputing facility.

References

[1] H.W. Kroto, J.R. Heath, S.C. O'Brien, R.F. Curl, R.E. Smalley, Nature (London) 318 (1985) 162.
[2] S. Iijima, Nature (London) 354 (1991) 56.
[3] N.G. Chopra, R.J. Luyken, K. Herrey, V.H. Crespi, M.L. Cohen, S.G. Louie, A. Zettl, Science 269 (1995) 966.
[4] X. Blasé, A. Rubio, S.G. Louie, M.L. Cohen, Europhys. Lett. 28 (1994) 335.
[5] L. Boulanger, B. Andriot, M. Cauchetier, F. Willaime, Chem. Phys. Lett. 234 (1995) 227.
[6] D. Golberg, Y. Bando, O. Stéphan, K. Kurashima, Appl. Phys. Lett. 73 (1998) 2441.
[7] F. Jensen, H. Toftlund, Chem. Phys. Lett. 201 (1993) 89.
[8] P.W. Fowler, T. Heine, D. Mitchell, R. Schmidt, G. Seifert, J. Chem. Soc. Farad. Trans. 92 (1996) 2197.
[9] G. Seifert, P.W. Flower, D. Mitchell, D. Porezag, Th. Frauenheim, Chem. Phys. Lett. 268 (1997) 352.
[10] S.S. Alexandre, H. Chacham, R.W. Nunes, Appl. Phys. Lett. 75 (1999) 61.
[11] T. Oku, M. Kuno, I. Narita, Diamond Rel. Mater. 11 (2002) 940.
[12] G. Kresse, J. Hafner, Phys. Rev. B 48 (1993) 13115.
[13] G. Kresse, J. Furthmüller, J. Comput. Mater. Sci. 6 (1996) 15.
[14] J.P. Perdew, Phys. Rev. B 46 (1992) 6671.
[15] P. Blöchl, Phys. Rev. B 50 (1994) 17953.
[16] G. Kresse, D. Joubert, Phys. Rev. B 59 (1999) 1758.